Synthetic-Aperture Assessment of a Dispersive Surface

Margaret Cheney
Department of Mathematical Sciences
Rensselaer Polytechnic Institute
Troy, NY 12180

This is a preprint of an articple published in *International Journal of Imaging Systems and Technology* 14 (2004) 28–34.

Abstract

This paper considers Synthetic Aperture Radar and other synthetic aperture imaging systems in which a backscattered wave is measured from a variety of locations. We focus on the case in which the ground-reflectivity function depends on frequency as well as on position.

The paper begins with a (linearized) mathematical model, based on a scalar approximation to Maxwell's equations, that includes the effects of the source waveform and the antenna beam pattern. The model can also accommodate other effects such as antenna steering and motion.

For this mathematical model, we use the tools of microlocal analysis to develop and analyze a three-dimensional inversion algorithm that uses measurements made on a surface and determines the frequency-dependent ground reflectivity.

1 Introduction

In Synthetic Aperture Radar (SAR) imaging [9] [10] [13], [14], a plane or satellite carrying an antenna moves along a flight path. The antenna emits pulses of electromagnetic radiation, which scatter off the terrain, and the scattered waves are detected with the same antenna. The received signals are then used to produce an image of the terrain. (See Figure 1)

Images of the ground reflectivity function are useful, but in some cases one wants more information. For example, in determining the extent and nature of chemical spills, it would be helpful to have information about the material properties of the

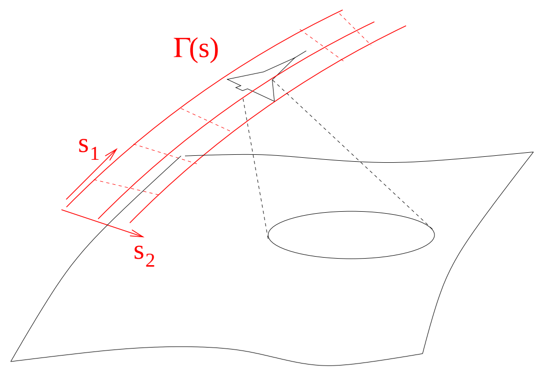

Figure 1: Geometry

ground. In this paper we consider the dispersive characteristics of the ground, i.e., the changes in reflectivity with frequency. The material properties then depend on three variables: frequency and position on a (known) surface.

In order to obtain a dataset that also depends on three variables, we consider the case in which multiple passes are made over the same scene, so that backscattered data is known for positions that sample a two-dimensional surface of sensor positions. The data then depend on three variables, namely time and position on the flight surface, so we expect to be able to reconstruct a function of three variables.

For the reconstruction, we use the methods of microlocal analysis [11] [15] [16] [33], which enable us to reconstruct the singularities in the scattering region [4] [3] [6] [21] [27][30]. Singularities correspond to edges and boundaries between different materials, so an image of the singularities gives us an image of structures such as walls and vehicles. The microlocal methods have the advantage of providing reconstruction formulas even in the case when the data is incomplete and non-ideal. In particular, these methods can accomodate the varying antenna beam patterns that arise in the cases of non-ideal antenna motion and gain, and with appropriate adjustments the same reconstruction formulas apply to both spotlight-mode [8] and stripmap-mode radar [9, 10] [14]. Microlocal reconstruction techniques have been used to advantage in the geophysics community, where they have been found to be fast and robust [4] [6].

Microlocal methods have two disadvantages. First, they apply only to linearized inverse problems. However, this is not a serious limitation for radar problems, since practically all work on radar already involves a linearization assumption. Second, microlocal methods can only be expected to provide a reconstruction of singularities and their strengths. For frequency-dependent scattering, we expect only that the high-frequency behavior of the material may be accurately reconstructed. However, in practice the microlocal techniques often give good results well beyond the regime in which they are expected to apply. In idealized cases where exact inversion formulas are known, the inversion formulas obtained by microlocal analysis typically reduce to these same exact inversion formulas.

In the paper we discuss explicitly the radar case, but the analysis applies equally well to sonar and ultrasound imaging.

2 The Mathematical model

2.1 A model for the wave propagation

For SAR, the correct model is Maxwell's equations, which we write as

$$\nabla \times \boldsymbol{E} = -\partial_t \boldsymbol{B} \tag{1}$$

$$\nabla \times \boldsymbol{H} = \boldsymbol{J} + \partial_t \boldsymbol{D} \tag{2}$$

$$\nabla \cdot \boldsymbol{D} = \rho \tag{3}$$

$$\nabla \cdot \boldsymbol{B} = 0 \tag{4}$$

Here $\boldsymbol{E}$ is the electric field, $\boldsymbol{H}$ the magnetic field, $\boldsymbol{D}$ the electric displacement, $\boldsymbol{B}$ the magnetic induction, $\boldsymbol{J}$ is the current density, and ρ is the charge density. The four fields $\boldsymbol{E}, \boldsymbol{D}, \boldsymbol{H}, \boldsymbol{B}$ are related by constitutive relations, which in this paper we assume to be of the form

$$\boldsymbol{B}(t,\boldsymbol{x}) = \mu_0 \boldsymbol{H}(t,\boldsymbol{x}) \tag{5}$$

$$\boldsymbol{D}(t,\boldsymbol{x}) = \int_0^\infty \varepsilon(t',\boldsymbol{x})\boldsymbol{E}(t-t',\boldsymbol{x})dt' \equiv (\varepsilon *_t \boldsymbol{E})(t,\boldsymbol{x}) \tag{6}$$

Here μ_0 is the magnetic permeability of free space, which means that we are considering non-magnetic materials. The relation between $\boldsymbol{D}$ and $\boldsymbol{E}$ is a causal convolution in time with the electric permittivity ϵ [18]. In general, the permittivity kernel is of the form $\varepsilon(t',\boldsymbol{x}) = \epsilon_\infty(\boldsymbol{x})\delta(t') + \chi_\epsilon(t',\boldsymbol{x})$ with χ_ϵ smooth; ϵ_∞ is called the *instantaneous response* and χ_ϵ is called the *susceptibility kernel*. Discontinuities in the electric and magnetic fields propagate with speed $c(\boldsymbol{x}) = 1/(\mu_0\epsilon_\infty(\boldsymbol{x}))^{1/2}$. Wave propagation in dispersive materials have been studied by a number of authors [20, 18, 19, 29, 31].

If we use (5) and (6) to eliminate $\boldsymbol{B}$ and $\boldsymbol{D}$ in (1) and (2), and then substitute the curl of (1) into (2), we obtain

$$\nabla \times \nabla \times \boldsymbol{E} = -\partial_t \mu_0 \boldsymbol{J} - \partial_{tt}(\mu_0 \varepsilon *_t \boldsymbol{E}). \tag{7}$$

Finally, we use the identity $\nabla \times \nabla \times \boldsymbol{E} = \nabla(\nabla \cdot \boldsymbol{E}) - \nabla^2 \boldsymbol{E}$ to write (7) as

$$\nabla^2 \boldsymbol{E} - \partial_{tt}(\mu_0 \varepsilon *_t \boldsymbol{E}) - \nabla(\nabla \cdot \boldsymbol{E}) = \mu_0 \partial_t \boldsymbol{J}. \tag{8}$$

Up to this point, our only assumptions have been (5) and (6); we now make a simplifying assumption to reduce (8) to three uncoupled scalar equations.

Assumption 1 We assume that $\nabla(\nabla \cdot \boldsymbol{E}) = 0$;

this reduces (8) to

$$\nabla^2 \boldsymbol{E} - \partial_{tt}(\mu_0 \varepsilon *_t \boldsymbol{E}) = \mu_0 \partial_t \boldsymbol{J}. \tag{9}$$

Assumption 1 does not hold in general; instead, from (3) and (6) we should have $\nabla \cdot (\varepsilon *_t \boldsymbol{E}) = \rho$. However, Assumption 1 holds within a homogeneous medium such as air. In general Assumption 1 does not hold at interfaces between materials; at such interfaces there is coupling between the different components of E. By using (9), we are ignoring such coupling, and we are thus ignoring polarization effects. Consequently we consider only one component of (9), thus reducing the problem to a scalar one.

We make the following assumptions about the nature of the scattering.

Assumption 2 The earth's surface $\mathcal{X} = \{\boldsymbol{x} = \boldsymbol{\psi}(\boldsymbol{x}_T) : \boldsymbol{x}_T \in \mathbb{R}^2\})$ is known and is well-separated from the flight paths, which lie on the surface $\Gamma(\boldsymbol{s})$, $\boldsymbol{s} \in \mathbb{R}^2$. In the region between the antenna and the earth's surface, the wave speed is $c_0 = 1/(\mu_0\epsilon_0)^{1/2}$. The scattering takes place in a thin region at the earth's surface. The scattering is due to a perturbation in the permittivity kernel at the earth's surface. This perturbation we write as $q(t', \boldsymbol{x}_T)\delta(\boldsymbol{x} - \boldsymbol{\psi}(\boldsymbol{x}_T)) = \mu_0[\epsilon(t', \boldsymbol{\psi}(\boldsymbol{x}_T)) - \epsilon_0\delta(t')]\delta(\boldsymbol{x} - \boldsymbol{\psi}(\boldsymbol{x}_T))$.

The equation we consider can thus be written

$$\nabla^2 E - c_0^{-2}\partial_{tt} E - \delta_\psi \partial_{tt}(q *_t E) = \mu_0 \partial_t J. \tag{10}$$

Here q, the *ground permittivity kernel*, is the quantity we wish to reconstruct. Its Fourier transform is the *frequency-dependent ground reflectivity function*

$$Q(\omega, \boldsymbol{x}_T) = \frac{1}{2\pi} \int e^{i\omega t} q(t, \boldsymbol{x}_T) dt. \tag{11}$$

2.2 A model for the field from an antenna

Between the antenna and the scattering surface, the scalar wave field E satisfies the free-space wave equation

$$\left(\nabla^2 - \frac{1}{c_0^2}\partial_{tt}\right) E = 0. \tag{12}$$

In free space, the field g_0 at t, x due to a delta function point source at the origin at time 0 is given by [32]

$$g_0(t, \boldsymbol{x}) = \frac{\delta(t - |\boldsymbol{x}|/c_0)}{4\pi|\boldsymbol{x}|} = \int \frac{e^{-i\omega(t - |\boldsymbol{x}|/c_0)}}{8\pi^2|\boldsymbol{x}|} d\omega, \tag{13}$$

which satisfies

$$\left(\nabla^2 - c_0^{-2}\partial_{tt}\right) g_0(t, \boldsymbol{x}) = -\delta(t)\delta(\boldsymbol{x}). \tag{14}$$

The antenna, however, is not a point source [34] $\delta(\boldsymbol{x})$, and the signal sent to the antenna is not a delta function $\delta(t)$. Therefore we replace $-\delta(t)\delta(\boldsymbol{x})$ by $-j_s(t,\boldsymbol{x})$, a quantity which is μ_0 times the time derivative of an effective current distribution over the antenna.

We write j_s in terms of its Fourier transform J_s:

$$j_s(t,\boldsymbol{x}) = \int e^{-i\omega t} J_s(\omega,\boldsymbol{x})d\omega, \tag{15}$$

where ω denotes the angular frequency. In practice, the waveform j_s is such that only a certain interval $0 < \omega_{\min} \leq \omega \leq \omega_{\max}$ contributes significantly to (15); we call this set the *effective support* of J_s. The difference $(\omega_{\max} - \omega_{\min})$ is the (angular-frequency) *bandwidth*. The fact that j_s is bandlimited means that ultimately we reconstruct bandlimited approximations to singularities rather than the actual singularities.

The field emanating from the antenna then satisfies

$$\left(\nabla^2 - c_0^{-2}\partial_{tt}\right) E^{in}(t,\boldsymbol{x}) = -j_s(t,\boldsymbol{x}) \tag{16}$$

so that

$$E^{in}(t,\boldsymbol{x}) = \int \frac{\delta(t-t'-|\boldsymbol{x}-\boldsymbol{y}|/c_0)}{4\pi|\boldsymbol{x}-\boldsymbol{y}|} j_s(t',\boldsymbol{y})dt'\, d\boldsymbol{y}. \tag{17}$$

With the notation (15), (17) becomes

$$E^{in}(t,\boldsymbol{x}) \;\; = \;\; \int \frac{e^{-i\omega(t-|\boldsymbol{x}-\boldsymbol{y}|/c_0)}}{4\pi|\boldsymbol{x}-\boldsymbol{y}|} J_s(\omega,\boldsymbol{y})d\omega d\boldsymbol{y}. \tag{18}$$

Next we assume that the antenna is small compared with the distance to the scatterers. We denote the center of the antenna by $\boldsymbol{y}^0$; thus a point on the antenna can be written $\boldsymbol{y} = \boldsymbol{y}^0 + \boldsymbol{y}'$, where $\boldsymbol{y}'$ is a vector from the center of the antenna to a point on the antenna. In this notation, the assumption that the scattering location $\boldsymbol{x}$ is far from the antenna can be expressed $|\boldsymbol{y}'| << |\boldsymbol{x}-\boldsymbol{y}^0|$. For such $\boldsymbol{x}$, we can write

$$|\boldsymbol{x}-\boldsymbol{y}| = |\boldsymbol{x}-\boldsymbol{y}^0| - (\widehat{\boldsymbol{x}-\boldsymbol{y}^0})\cdot\boldsymbol{y}' + O(|\boldsymbol{y}'|^2/|\boldsymbol{x}-\boldsymbol{y}^0|), \tag{19}$$

where $\hat{\boldsymbol{y}}$ denotes a unit vector in the same direction as $\boldsymbol{y}$.

We use the expansion (19) in (18) to obtain

$$\begin{aligned} E^{in}(t,\boldsymbol{x}) &\approx \int \frac{e^{-i\omega(t-|\boldsymbol{x}-\boldsymbol{y}^0|/c_0)}}{4\pi|\boldsymbol{x}-\boldsymbol{y}^0|} e^{-i\omega(\widehat{\boldsymbol{x}-\boldsymbol{y}^0})\cdot\boldsymbol{y}'} J_s(\omega,\boldsymbol{y}^0+\boldsymbol{y}')d\omega d\boldsymbol{y}' \\ &\approx \int \frac{e^{-i\omega(t-|\boldsymbol{x}-\boldsymbol{y}^0|/c_0)}}{4\pi|\boldsymbol{x}-\boldsymbol{y}^0|} \hat{J}_s(\omega,\omega(\widehat{\boldsymbol{x}-\boldsymbol{y}^0}),\boldsymbol{y}^0)d\omega \end{aligned} \tag{20}$$

where we have written

$$\hat{J}_s(\omega(\widehat{\boldsymbol{x}-\boldsymbol{y}^0}),\boldsymbol{y}^0) \;\; = \;\; \int e^{-i\omega(\widehat{\boldsymbol{x}-\boldsymbol{y}^0})\cdot\boldsymbol{y}'} J_s(\omega,\boldsymbol{y}^0+\boldsymbol{y}')d\boldsymbol{y}'$$

$$= e^{i\omega(\widehat{\boldsymbol{x}-\boldsymbol{y}^0})\cdot\boldsymbol{y}^0} \int e^{-i\omega(\widehat{\boldsymbol{x}-\boldsymbol{y}^0})\cdot\boldsymbol{v}} J_s(\omega,\boldsymbol{v})d\boldsymbol{v} \qquad (21)$$

This Fourier transform of the current density thus gives the antenna beam pattern in the far-field at each fixed frequency.

We see from (20) that the field emanating from the antenna is a superposition of fixed-frequency point sources that are each shaped by the antenna beam pattern. We note that the field (20) clearly depends on $\boldsymbol{y}^0$, the location of the center of the antenna.

2.3 A linearized scattering model

We rewrite (9) by making the change of variables $t' \to t - t'$ in the convolution integral:

$$\nabla^2 E(t,\boldsymbol{x}) - c_0^{-2}\partial_{tt}E(t,\boldsymbol{x}) = \delta(\boldsymbol{x}-\boldsymbol{\psi}(\boldsymbol{x}_T)) \int q(t-t',\boldsymbol{x}_T)\ddot{E}(t',\boldsymbol{x})dt' - j_s(t,\boldsymbol{x}), \qquad (22)$$

where the dots denote differentiation with respect to t'. We write $E = E^{in} + E^{sc}$ in (22) and use (16) to obtain

$$\left(\nabla^2 - c_0^{-2}\partial_{tt}\right) E^{sc}(t,\boldsymbol{x}) = \delta(\boldsymbol{x}-\boldsymbol{\psi}(\boldsymbol{x}_T)) \int q(t-t',\boldsymbol{x}_T)\ddot{E}(t',\boldsymbol{x})dt'. \qquad (23)$$

We can write (23) as an integral equation

$$E^{sc}(t,\boldsymbol{x}) = -\int g_0(t-t',\boldsymbol{x}-\boldsymbol{z})\delta(\boldsymbol{z}-\boldsymbol{\psi}(\boldsymbol{z}_T)) \int q(t'-t'',\boldsymbol{z}_T)\ddot{E}(t'',\boldsymbol{z})dt''dt'd\boldsymbol{z}. \qquad (24)$$

A commonly used approximation [20] [17], often called the *Born approximation* or the *single scattering approximation*, is to replace the full field E on the right side of (24) and (23) by the incident field E^{in}, which converts (24) to

$$E_B^{sc}(t,\boldsymbol{x}) \approx -\int g_0(t-t',\boldsymbol{x}-\boldsymbol{\psi}(\boldsymbol{z}_T)) \int q(t'-t'',\boldsymbol{z}_T)\ddot{E}^{in}(t'',\boldsymbol{\psi}(\boldsymbol{z}_T))dt''dt'd\boldsymbol{z}_T \qquad (25)$$

The value of this approximation is that it removes the nonlinearity in the inverse problem: it replaces the product of two unknowns (q and E) by a single unknown (q) multiplied by the known incident field.

The Born approximation makes the problem simpler, but it is not necessarily a good approximation. Another linearizing approximation that can be used for reflection from smooth surfaces is the *Kirchhoff approximation*, in which the scattered field is replaced by its geometrical optics approximation [6] [20]. Here, however, we consider only the Born approximation.

For the incident field (20) with antenna center $\boldsymbol{y}^0 = \boldsymbol{\Gamma}$, the Born-approximated field $E_B^{sc}(t,\boldsymbol{x},\boldsymbol{\Gamma})$ of (25) becomes

$$E_B^{sc}(t,\boldsymbol{x},\boldsymbol{\Gamma}) = -\int\int \frac{e^{-i\omega(t-t'-|\boldsymbol{x}-\boldsymbol{\psi}(\boldsymbol{z}_T)|/c_0)}}{4\pi|\boldsymbol{x}-\boldsymbol{\psi}(\boldsymbol{z}_T)|}d\omega \int q(t'-t'',\boldsymbol{\psi}(\boldsymbol{z}_T))$$

$$\times \int (-i\omega')^2 \frac{e^{-i\omega'(t''-|\boldsymbol{\psi}(\boldsymbol{z})-\boldsymbol{\Gamma}|/c_0)}}{4\pi|\boldsymbol{\psi}(\boldsymbol{z}_T)-\boldsymbol{\Gamma}|} \hat{J}_s(\omega', \omega'(\widehat{\boldsymbol{\psi}(\boldsymbol{z}_T)-\boldsymbol{\Gamma}}), \boldsymbol{\Gamma}) d\omega' dt'' dt' d\boldsymbol{z}_T \tag{26}$$

In this equation, we make the substitution $\tilde{t} = t' - t''$ and carry out the t' integration. The result is

$$\begin{aligned} E_B^{sc}(t, \boldsymbol{x}, \boldsymbol{\Gamma}) &= \int\int \frac{e^{-i\omega[t-\tilde{t}-(|\boldsymbol{x}-\boldsymbol{\psi}(\boldsymbol{z}_T)|+|\boldsymbol{\psi}(\boldsymbol{z}_T)-\boldsymbol{\Gamma}|)/c_0]}}{4\pi||\boldsymbol{x}-\boldsymbol{\psi}(\boldsymbol{z}_T)|4\pi|\boldsymbol{\psi}(\boldsymbol{z}_T)-\boldsymbol{\Gamma}|} \int q(\tilde{t}, \boldsymbol{\psi}(\boldsymbol{z}_T)) \\ &\quad \times \hat{J}_s(\omega, \omega(\widehat{\boldsymbol{\psi}(\boldsymbol{z}_T)-\boldsymbol{\Gamma}}), \boldsymbol{\Gamma}) \omega^2 d\omega d\tilde{t} d\boldsymbol{z}_T. \end{aligned} \tag{27}$$

2.4 The received signal

When the scattered field is received back at the antenna, the effect is to convolve the field with some weight $j_r(t, \boldsymbol{\Gamma} + \boldsymbol{y}')$, so that the measured signal is

$$\begin{aligned} \int E^{sc} *_t j_r d\boldsymbol{y}' &\approx \int E_B^{sc}(t-t', \boldsymbol{\Gamma}+\boldsymbol{y}', \boldsymbol{\Gamma}) j_r(t', \boldsymbol{\Gamma}+\boldsymbol{y}') dt' d\boldsymbol{y}' \\ &= \int\int\int \frac{e^{-i\omega[t-t'-\tilde{t}-(|\boldsymbol{\Gamma}+\boldsymbol{y}'-\boldsymbol{\psi}(\boldsymbol{z}_T)|+|\boldsymbol{\psi}(\boldsymbol{z}_T-\boldsymbol{\Gamma}|)/c_0]}}{4\pi|\boldsymbol{\Gamma}+\boldsymbol{y}'-\boldsymbol{\psi}(\boldsymbol{z}_T)|4\pi|\boldsymbol{\psi}(\boldsymbol{z}_T)-\boldsymbol{\Gamma}|} \int q(\tilde{t}, \boldsymbol{\psi}(\boldsymbol{z}_T)) \\ &\quad \times \hat{J}_s(\omega, \omega(\widehat{\boldsymbol{\psi}(\boldsymbol{z}_T)-\boldsymbol{\Gamma}}), \boldsymbol{\Gamma}) \omega^2 d\omega d\tilde{t} d\boldsymbol{z}_T j_r(t', \boldsymbol{\Gamma}+\boldsymbol{y}') dt' d\boldsymbol{y}'; \end{aligned} \tag{28}$$

(Normally, when the same antenna is used for transmission and reception, $j_r = j_s$.)

As before, we make the far-field approximation and write the receiver weighting pattern $j_r(t, \boldsymbol{\Gamma} + \boldsymbol{y}')$ in terms of its temporal Fourier transform. Thus a model for the received signal S is

$$\begin{aligned} S(t, \boldsymbol{\Gamma}) &= \int\int\int \frac{e^{-i\omega[t-\tilde{t}-2|\boldsymbol{\Gamma}-\boldsymbol{\psi}(\boldsymbol{z}_T)|/c_0]}}{(4\pi)^2|\boldsymbol{\Gamma}-\boldsymbol{\psi}(\boldsymbol{z}_T)|^2} \int q(\tilde{t}, \boldsymbol{\psi}(\boldsymbol{z}_T)) \\ &\quad \times \hat{J}_s(\omega, \omega(\widehat{\boldsymbol{\psi}(\boldsymbol{z}_T)-\boldsymbol{\Gamma}}), \boldsymbol{\Gamma}) \hat{J}_r(\omega, \omega(\widehat{\boldsymbol{\psi}(\boldsymbol{z}_T)-\boldsymbol{\Gamma}}), \boldsymbol{\Gamma}) \omega^2 d\omega d\tilde{t} d\boldsymbol{z}_T \end{aligned} \tag{29}$$

The idealized inverse problem is to determine q from knowledge of S for all t and for $\boldsymbol{\Gamma}$ on a surface. This surface we parametrize by $\{\boldsymbol{\Gamma}(\boldsymbol{s}) : \boldsymbol{s} = (s_1, s_2), \text{where } s_1^{\min} < s_1 < s_1^{\max},\ s_2^{\min} < s_2 < s_2^{\max}\}$.

The abrupt edges of the surface $\boldsymbol{\Gamma}$ tend to cause artifacts in the image [28]; consequently it is useful to multiply the data by a smooth taper function $m(t, \boldsymbol{s})$ supported in $(t, \boldsymbol{s}) \in [0, T] \times [s_1^{\min}, s_1^{\max}] \times [s_2^{\min}, s_2^{\max}]$.

We write the data as $d(t, \boldsymbol{s}) = m(t, \boldsymbol{s}) S(t, \boldsymbol{\Gamma}(\boldsymbol{s}))$; we denote the map from scene q to data d by F, so that

$$d(t, \boldsymbol{s}) = F[q](t, \boldsymbol{s}) = \int e^{-i\omega(t-t'-2R(\boldsymbol{s},\boldsymbol{z}_T)/c_0)} A(t, \boldsymbol{s}, \boldsymbol{z}_T, \omega) q(t', \boldsymbol{z}_T)\, d\omega dt' d\boldsymbol{z}_T, \tag{30}$$

where

$$A(t,\boldsymbol{s},\boldsymbol{z}_T,\omega) = \frac{\omega^2 \hat{J}_s(\omega,\omega\hat{\boldsymbol{R}}(\boldsymbol{s},\boldsymbol{z}_T),\boldsymbol{\Gamma}(\boldsymbol{s}))\hat{J}_r(\omega,\omega\hat{\boldsymbol{R}}(\boldsymbol{s},\boldsymbol{z}_T),\boldsymbol{\Gamma}(\boldsymbol{s}))m(t,\boldsymbol{s})}{(4\pi)^2 R(\boldsymbol{x},\boldsymbol{z}_T)^2} \tag{31}$$

and where $\boldsymbol{R}(\boldsymbol{s},\boldsymbol{z}_T) = |\boldsymbol{\Gamma}(\boldsymbol{s}) - \boldsymbol{\psi}(\boldsymbol{z}_T)|$, $R = |\boldsymbol{R}|$, and $\hat{\boldsymbol{R}} = \boldsymbol{R}/R$. In practice, the measured signal is subject to a variety of other effects, such as antenna steerng and motion; these effects are included through the $\boldsymbol{s}$-dependence of the antenna beam pattern.

We assume

Assumption 3 The amplitude A of (30) satisfes

$$\sup_{(s,t,x)\in K} |\,\partial_\omega^\alpha \partial_{s_1}^{\beta_1}\partial_{s_2}^{\beta_2}\partial_t^\delta \partial_{x_1}^{\rho_1}\partial_{x_2}^{\rho_2} A(t,\boldsymbol{s},\boldsymbol{z}_T,\omega)\,| \le C_{K,\alpha,\boldsymbol{\beta},\delta,\boldsymbol{\rho}}(1+\omega^2)^{(2-|\alpha|)/2} \tag{32}$$

where K is any compact set, $\boldsymbol{\rho} = (\rho_1,\rho_2)$, $|\boldsymbol{\rho}| = \rho_1 + \rho_2$, and similarly for $\boldsymbol{\beta}$.

This assumption is true for example when the antenna is broadband and the source waveform is a delta function or band-limited waveform. Under this assumption, the "forward" operator F is an example of a Fourier Integral Operator [11], [33], [15].

3 Image formation

We form the image I by means of a *filtered backprojection* operator:

$$I(t,\boldsymbol{x}_T) = B[d](t,\boldsymbol{x}_T) := \int b(t,\boldsymbol{s},\boldsymbol{x}_T,\omega)e^{i\omega(t'-t-2R(\boldsymbol{s},\boldsymbol{x}_T)/c_0)}d(t',\boldsymbol{s})\, d\omega d\boldsymbol{s} dt', \tag{33}$$

where B is determined below. We note that the spatial part of this backprojection operator is a filtered version of the adjoint of spatial part of F, but that the temporal part has the opposite sign.

To determine b, we investigate the degree to which the image I faithfully reproduces features of the ground permittivity kernel q. We will show that under favorable circumstances, singular features such as edges appear in the correct locations.

Using $d = F[V]$ in (33) results in an equation of the form

$$I(t,\boldsymbol{x}_T) = \int K(t,\boldsymbol{x}_T,t'',\boldsymbol{z}_T)q(t'',\boldsymbol{z}_T)dt''d\boldsymbol{z}_T, \tag{34}$$

where

$$K(t,\boldsymbol{x}_T,t'',\boldsymbol{z}_T) = \int e^{i\omega(t'-t-2R(\boldsymbol{s},\boldsymbol{x}_T)|/c_0)}e^{-i\omega'(t'-t''-2R(\boldsymbol{s},\boldsymbol{z}_T)/c_0)} b(t,\boldsymbol{s},\boldsymbol{x}_T,\omega)A(t',\boldsymbol{s},\boldsymbol{z}_T,\omega')\, d\omega'\, d\omega\, d\boldsymbol{s}\, dt', \tag{35}$$

The kernel K is the imaging *point-spread function*. If we had $K(t, \boldsymbol{x}_T, t'', \boldsymbol{z}_T) = \delta(\boldsymbol{z}_T - \boldsymbol{x}_T)\delta(t - t'')$, then the image I would be perfect; we want to determine b so that K comes as close as possible to being a delta function.

In (35), we perform a large-ω stationary phase calculation in the variables ω' and t'. (Specifically, we make the change of variables $\tilde{\omega} = \omega v$ and perform a large-ω stationary phase calculation in the variables v and t'; the result is the same as if we had used $\int \exp[it'(\omega - \omega')]dt' = 2\pi\delta(\omega - \omega')$ and set $t' = t'' - 2R(\boldsymbol{s}, \boldsymbol{z}_T)/c_0$. A statement of the multi-dimensional stationary phase theorem is given in the Appendix.)

After substituting the stationary phase result into (35), we obtain

$$K(t, \boldsymbol{x}_T, t'', \boldsymbol{z}_T) = 2\pi \int e^{i\omega[t'' - t + 2(R(\boldsymbol{s}, \boldsymbol{z}_T) - R(\boldsymbol{s}, \boldsymbol{x}_T))/c_0]} b(t, \boldsymbol{s}, \boldsymbol{x}_T, \omega) \\ A(t'(t'', \boldsymbol{s}, \boldsymbol{z}_T), \boldsymbol{s}, \boldsymbol{z}_T, \omega)\, d\omega\, d\boldsymbol{s} + E_1, \qquad (36)$$

where $t'(t'', \boldsymbol{s}, \boldsymbol{z}_T) = t'' - 2R(\boldsymbol{s}, \boldsymbol{z}_T)/c_0$ and where E_1 denotes a function smoother than the first term on the right side of (36).

If K is to be a delta function, then certainly at the critical points of (36), we should have $\boldsymbol{x}_T = \boldsymbol{z}_T$ and $t = t''$. From differentiating the phase of (36) with respect to ω and $\boldsymbol{s}$, we find that the critical points must satisfy

$$t'' - t = \frac{2}{c_0}[R(\boldsymbol{s}, \boldsymbol{z}_T) - R(\boldsymbol{s}, \boldsymbol{x}_T)] \\ [\hat{R}(\boldsymbol{s}, \boldsymbol{z}_T) - \hat{R}(\boldsymbol{s}, \boldsymbol{x}_T)] \cdot \frac{\partial \boldsymbol{\Gamma}}{\partial s_j} = 0, \qquad j = 1, 2 \qquad (37)$$

The second line of (37) says that two components of $\hat{R}(\boldsymbol{s}, \boldsymbol{x}_T)$ and $\hat{R}(\boldsymbol{s}, \boldsymbol{z}_T)$ must be the same. If the flight paths are roughly horizontal, since $\hat{R}(\boldsymbol{s}, \boldsymbol{x}_T)$ and $\hat{R}(\boldsymbol{s}, \boldsymbol{z}_T)$ are unit vectors and are both pointing downwards, they must be identical. (In certain pathological cases, such as when the measurement surface $\boldsymbol{\Gamma}$ is perpendicular to the earth's surface, it is possible for $\hat{R}(\boldsymbol{s}, \boldsymbol{x}_T)$ and $\hat{R}(\boldsymbol{s}, \boldsymbol{z}_T)$ to have their third components of opposite sign.)

When $\hat{R}(\boldsymbol{s}, \boldsymbol{x}_T)$ and $\hat{R}(\boldsymbol{s}, \boldsymbol{z}_T)$ are identical, then since the ground surface ψ is known, $\boldsymbol{x}_T$ and $\boldsymbol{z}_T$ must also be identical. (Here again we exclude pathological cases such as the radar lying in the tangent plane to the ground.) When $\boldsymbol{x}_T = \boldsymbol{z}_T$, then $\hat{R}(\boldsymbol{s}, \boldsymbol{x}_T) = \hat{R}(\boldsymbol{s}, \boldsymbol{z}_T)$, and the first line of (37) implies that $t = t''$. Thus the leading order contributions to (36) are from points with $\boldsymbol{x}_T = \boldsymbol{z}_T$ and $t = t''$.

3.1 Determination of b

In the exponent of (36), we use the identity

$$f(\boldsymbol{x}) - f(\boldsymbol{y}) = \int_0^1 \frac{d}{d\lambda} f(\boldsymbol{y} + \lambda(\boldsymbol{x} - \boldsymbol{y}))d\lambda = (\boldsymbol{x} - \boldsymbol{y}) \cdot \int_0^1 (\nabla f)(\boldsymbol{y} + \lambda(\boldsymbol{x} - \boldsymbol{y}))d\lambda \quad (38)$$

to write

$$\omega[t'' - t + 2(R(\boldsymbol{s}, \boldsymbol{z}_T) - R(\boldsymbol{s}, \boldsymbol{x}_T))/c_0] = -(t - t'')\omega + (\boldsymbol{z}_T - \boldsymbol{x}_T) \cdot \Xi(\boldsymbol{z}_T, \boldsymbol{x}_T, \boldsymbol{s}, \omega); \tag{39}$$

explicitly, Ξ is given by

$$\Xi_j(\boldsymbol{z}_T, \boldsymbol{x}_T, \boldsymbol{s}, \omega) = \frac{2\omega}{c_0} \int_0^1 \hat{\boldsymbol{R}}(\boldsymbol{s}, \boldsymbol{y}) \cdot \frac{\partial \boldsymbol{\psi}}{\partial y_j}\bigg|_{\boldsymbol{y}_T = \boldsymbol{x}_T + \lambda(\boldsymbol{z}_T - \boldsymbol{x}_T)} d\lambda; \tag{40}$$

when $\boldsymbol{z}_T = \boldsymbol{x}_T$, it is simply

$$\Xi_j(\boldsymbol{z}_T, \boldsymbol{z}_T, \boldsymbol{s}, \omega) = \frac{2\omega}{c_0} \hat{\boldsymbol{R}}(\boldsymbol{s}, \boldsymbol{z}_T) \cdot \frac{\partial \boldsymbol{\psi}}{\partial z_j}. \tag{41}$$

In (36), we make the change of variables

$$(\omega, \boldsymbol{s}) \to (\tau, \boldsymbol{\xi}) = (-\omega, \Xi(\boldsymbol{z}_T, \boldsymbol{x}_T, \boldsymbol{s}, \omega)). \tag{42}$$

This transforms the integral (36) into

$$K(t, \boldsymbol{x}_T, t'', \boldsymbol{z}_T) = 2\pi \int e^{i[(t-t'')\tau + (\boldsymbol{x}_T - \boldsymbol{z}_T)\cdot \boldsymbol{\xi}]} b(t, \boldsymbol{s}, \boldsymbol{x}_T, \omega) A(t'(t'', \boldsymbol{s}, \boldsymbol{z}_T), \boldsymbol{s}, \boldsymbol{z}_T, \omega) \left| \det \left(\frac{\partial(\omega, \boldsymbol{s})}{\partial(\tau, \boldsymbol{\xi})} \right)_{(\boldsymbol{z}_T, \boldsymbol{x}_T, \boldsymbol{s}, \omega)} \right| d\tau d\boldsymbol{\xi} + E_1, \tag{43}$$

where $\boldsymbol{s} = \boldsymbol{s}(\boldsymbol{\xi})$ and $\omega = \omega(\boldsymbol{\xi})$.

Equation (43) exhibits the point spread function K as the kernel of a pseudodifferential operator. Pseudodifferential operators have the *pseudolocal* property [33], i.e., they do not move singularities or change their orientation. It is immediately clear from (43) that provided the Jacobian $|\partial(\omega, \boldsymbol{s})/\partial\Xi|$ is nonzero, the leading order contribution to the image comes from the points $t = t'', \boldsymbol{x}_T = \boldsymbol{z}_T$.

We see from (43) that the backprojection weighting function b should be chosen as

$$b(t, \boldsymbol{s}, \boldsymbol{x}_T, \omega) = \frac{\left| \det \left(\frac{\partial(\tau, \boldsymbol{\xi})}{\partial(\omega, \boldsymbol{s})} \right)_{(\boldsymbol{x}_T, \boldsymbol{x}_T, \boldsymbol{s}, \omega)} \right| \chi(t, \boldsymbol{s}, \boldsymbol{x}, \omega)}{A(t'(t, \boldsymbol{s}, \boldsymbol{x}_T), \boldsymbol{s}, \boldsymbol{x}_T, \omega)} \tag{44}$$

where χ is a smooth cutoff function that prevents division by zero in (44).

The Jacobian determinant $|\partial(\omega, \boldsymbol{s})/\partial\Xi|$ is called the *Beylkin determinant* [4] [6]. To compute it at $\boldsymbol{x}_T = \boldsymbol{z}_T$, we first calculate the Jacobian matrix

$$\frac{\partial(\tau, \boldsymbol{\xi})}{\partial(\omega, \boldsymbol{s})} = \begin{pmatrix} -1 & 0 & 0 \\ \frac{2}{c}\hat{\boldsymbol{R}} \cdot \frac{\partial \boldsymbol{\psi}}{\partial x_1} & (P\frac{\partial \boldsymbol{\Gamma}}{\partial s_1}) \cdot \frac{\partial \boldsymbol{\psi}}{\partial x_1} & (P\frac{\partial \boldsymbol{\Gamma}}{\partial s_2}) \cdot \frac{\partial \boldsymbol{\psi}}{\partial x_1} \\ \frac{2}{c}\hat{\boldsymbol{R}} \cdot \frac{\partial \boldsymbol{\psi}}{\partial x_2} & (P\frac{\partial \boldsymbol{\Gamma}}{\partial s_1}) \cdot \frac{\partial \boldsymbol{\psi}}{\partial x_2} & (P\frac{\partial \boldsymbol{\Gamma}}{\partial s_2}) \cdot \frac{\partial \boldsymbol{\psi}}{\partial x_2} \end{pmatrix} \tag{45}$$

where P is the projection operator that projects a vector onto the plane perpendicular to $\hat{\boldsymbol{R}}$:

$$P\boldsymbol{v} = \frac{\boldsymbol{v} - \hat{\boldsymbol{R}}(\hat{\boldsymbol{R}} \cdot \boldsymbol{v})}{|\boldsymbol{R}|}. \tag{46}$$

From (45), it is easy to calculate the determinant:

$$\det\left(\frac{\partial(\tau, \boldsymbol{\xi})}{\partial(\omega, \boldsymbol{s})}\right) = \begin{vmatrix} (P\frac{\partial \boldsymbol{\Gamma}}{\partial s_1}) \cdot \frac{\partial \boldsymbol{\psi}}{\partial x_1} & (P\frac{\partial \boldsymbol{\Gamma}}{\partial s_2}) \cdot \frac{\partial \boldsymbol{\psi}}{\partial x_1} \\ (P\frac{\partial \boldsymbol{\Gamma}}{\partial s_1}) \cdot \frac{\partial \boldsymbol{\psi}}{\partial x_2} & (P\frac{\partial \boldsymbol{\Gamma}}{\partial s_2}) \cdot \frac{\partial \boldsymbol{\psi}}{\partial x_2} \end{vmatrix}. \tag{47}$$

This determinant is zero only when the two vectors $P(\partial\boldsymbol{\Gamma}/\partial s_1)$ and $P(\partial\boldsymbol{\Gamma}/\partial s_2)$, when projected onto the tangent plane to the earth's surface at $\boldsymbol{x}_T$, are linearly dependent. This would happen, for example, if the measurement surface $\boldsymbol{\Gamma}$ is perpendicular to the earth's surface.

3.2 Implementation

The formula (33) might be implemented numerically by a) applying a fast Fourier transform in the t' variable to $d(t', \boldsymbol{s})$ to obtain $D(\omega, \boldsymbol{s})$; b) for each $\boldsymbol{s}$ and each point $(t, \boldsymbol{x}_T)$ in the image, multiply D by the filter $b(t, \boldsymbol{s}, \boldsymbol{x}_T, \omega)$ defined by (44); d) inverse Fourier transform bD and evaluate the result at $t - 2R(\boldsymbol{s}, \boldsymbol{x}_T)/c_0$ to obtain the backprojected image from one antenna position; and finally e) sum over all antenna positions $\boldsymbol{s}$. A faster algorithm might be developed by following the ideas developed in [22, 1, 2].

The resolution of the resulting image is determined by the degree to which K approximates a delta function, which is determined by the support of χ, which is in turn determined though (41) by the overall size of the measurement surface $\boldsymbol{\Gamma}$.

4 Conclusions

To image a frequency-dependent ground-reflectivity function, we need to collect data that depends on three variables: time and two spatial variables. An image can be formed by applying the operator (33), where b is given by (44). This procedure gives a three-dimensional “image” of q, in which the third dimension is time. In this image, the visible singularities appear with the correct position, orientation, and strength. To obtain the frequency-dependent ground reflectivity function, q should be Fourier transformed via (11). The resulting Q we expect to be accurate in its high-frequency asymptotics.

5 Acknowledgments

I am grateful to Richard Albanese for suggesting the problem, and to the Air Force Office of Scientific Research[1] for supporting this work under agreement number F49620-03-1-0051. This work was also supported in part by the National Science Foundation through its Engineering Research Centers Program (award number EEC-9986821) and its Focused Research Groups in the Mathematical Sciences program. I thank Cliff Nolan for Figure 1.

A The Stationary Phase Theorem

The stationary phase theorem states [15] [5] [16]

Theorem A.1 If a is a smooth function of compact support on $\mathbf{R^n}$, and ϕ has only non-degenerate critical points, then as $\omega \to \infty$,

$$\int e^{i\omega\phi(\boldsymbol{x})} a(\boldsymbol{x}) d^n\boldsymbol{x} = \sum_{\{\boldsymbol{x}^0 : D\phi(\boldsymbol{x}^0)=\mathbf{0}\}} \left(\frac{2\pi}{\omega}\right)^{n/2} a(\boldsymbol{x}^0) \frac{e^{i\omega\phi(\boldsymbol{x}^0)} e^{i(\pi/4)\operatorname{sgn} D^2\phi(\boldsymbol{x}^0)}}{\sqrt{|\det D^2\phi(\boldsymbol{x}^0)|}} + O(\omega^{-n/2-1}) \quad (48)$$

Here $D\phi$ denotes the gradient of ϕ, $D^2\phi$ denotes the Hessian, and sgn denotes the signature of a matrix, i.e., the number of positive eigenvalues minus the number of negative ones.

B Composition of Fourier Integral Operators

In section 3, we determine the weight b by composing the two Fourier integral operators (FIOs) B and F; however arbitrary FIOs cannot necessarily be sensibly composed with each other. Conditions under which the composition is again an FIO are given in [11]; these conditions involve the (twisted) *canonical relation* computed from the phase function of the FIO. For an FIO of the form

$$Af(\boldsymbol{y}) = \int\int e^{i\phi(\boldsymbol{y},\boldsymbol{x},\omega)} a(\boldsymbol{y},\boldsymbol{x},\omega) f(x) d\omega d\boldsymbol{x}, \quad (49)$$

the (twisted) canonical relation is

$$\Lambda'_A = \{((\boldsymbol{y},\boldsymbol{\eta}),(\boldsymbol{x},\boldsymbol{\xi})) : d_\omega\phi(\boldsymbol{y},\boldsymbol{x},\omega) = 0, \boldsymbol{\eta} = \nabla_{\boldsymbol{y}}\phi(\boldsymbol{y},\boldsymbol{x},\omega), \boldsymbol{\xi} = -\nabla_{\boldsymbol{x}}\phi(\boldsymbol{y},\boldsymbol{x},\omega)\}. \quad (50)$$

[1]Consequently the U.S. Government is authorized to reproduce and distribute reprints for Governmental purposes notwithstanding any copyright notation thereon. The views and conclusions contained herein are those of the authors and should not be interpreted as necessarily representing the official policies or endorsements, either expressed or implied, of the Air Force Research Laboratory or the U.S. Government.

The main conditions we need to check [11] under which the composition BA is an FIO are that whenever $((\boldsymbol{z},\boldsymbol{\zeta}),(\boldsymbol{y},\boldsymbol{\eta}))\in\Lambda'_B$ and $((\boldsymbol{y},\boldsymbol{\eta}),(\boldsymbol{x},\boldsymbol{\xi}))\in\Lambda'_A$, we must have $\boldsymbol{\eta}\neq\mathbf{0}$ and either $\boldsymbol{\zeta}\neq\mathbf{0}$ or $\boldsymbol{\xi}\neq\mathbf{0}$.

In the case of $A=F$ (30) and B given by (33), the role of $\boldsymbol{y}$ is played by $(t,\boldsymbol{s})$, the role of $\boldsymbol{x}$ is played by $(t',\boldsymbol{x}_T)$, the phase function ϕ is $\phi(t,t',\boldsymbol{s},\boldsymbol{x}_T,\omega)=\omega(t-t'-2|\boldsymbol{\Gamma}(\boldsymbol{s})-\psi(\boldsymbol{x}_T)|/c_0)$, and the phase of B is just the negative of ϕ. This implies that $\boldsymbol{\eta}=(\omega,\nabla_{\boldsymbol{s}}\phi)$. Since for any radar system $\omega_{\min}$ is greater than zero, $\boldsymbol{\eta}$ is never zero. Similarly, $\boldsymbol{\xi}=(\omega,2\omega(\widehat{\Gamma(s)-\psi(\mathbf{x_T})})\cdot D\boldsymbol{\psi}/c_0)$ is never zero because ω is never zero. Thus the composition BF is an FIO.

References

[1] S. Basu and Y. Bressler, "$O(N^2\log_2 N)$ filtered backprojection reconstruction algorithm for tomography", IEEE Trans. Image Processing 9 (2000) 1760–1773.

[2] S. Basu and Y. Bressler, "Error analysis and performance optimization of fast hierarchical backrpojection algorithms" IEEE Trans. Image Processing 10 (2001) 1103–1117.

[3] G. Beylkin and R. Burridge, "Linearized inverse scattering problems in acoustics and elasticity", Wave Motion 12 (1990) 15–52.

[4] G. Beylkin, "Imaging of discontinuities in the inverse scattering problem by inversion of a causal generalized Radon transform", J. Math. Phys., 26 (1985) 99–108.

[5] N. Bleistein and R.A. Handelsman, Asymptotic Expansions of Integrals, Dover, New York, 1986.

[6] N. Bleistein, J. K. Cohen, and J.W. Stockwell, The Mathematics of Multidimensional Seismic Inversion, Springer, New York, 2000.

[7] M. Cheney, "A mathematical tutorial on Synthetic Aperture Radar", SIAM Review 43 (2001) 301–312.

[8] W. C. Carrara, R. G. Goodman, R. M. Majewski, Spotlight Synthetic Aperture Radar: Signal Processing Algorithms, Artech House, Boston, 1995.

[9] J.C. Curlander and R.N. McDonough, Synthetic Aperture Radar, Wiley, New York, 1991.

[10] L.J. Cutrona, "Synthetic Aperture Radar", in Radar Handbook, second edition, ed. M. Skolnik, McGraw-Hill, New York, 1990.

[11] J.J. Duistermaat, Fourier Integral Operators, Birkhauser, Boston, 1996.

[12] I. Egorov, "Second forerunners in reflection and transmission data", J. Opt. A Pure Appl. Opt. 1(1) (1999) 51–59.

[13] C. Elachi, Spaceborne Radar Remote Sensing: Applications and Techniques, IEEE Press, New York, 1987.

[14] G. Franceschetti and R. Lanari, Synthetic Aperture Radar Processing, CRC Press, New York, 1999.

[15] A. Grigis and J. Sjöstrand, Microlocal Analysis for Differential Operators: An Introduction, London Mathematical Society Lecture Note Series vol. 196, Cambridge University Press, 1994.

[16] V. Guillemin and S. Sternberg, Geometric Asymptotics, American Math. Society, Providence, 1979.

[17] G. T. Herman, and H. K. Tuy, K.J. Langenberg and P.C. Sabatier, Basic methods of tomography and inverse problems, Adam Hilger, Phildelphia, 1988.

[18] A. Karlsson and G. Kristensson, "Constitutive relations, dissipation and reciprocity for the Maxwell equations in the time domain", J. Electro. Waves Applic., 6(5/6) (1992) 537–551.

[19] A. Karlsson and S. Rikte, "The time-domain theory of forerunners", J. Opt. Soc. Am. A 15(2) (1998) 487-502.

[20] R.M. Lewis, "Asymptotic theory of wave-propagation", Arch. Rational Mech. Anal. 20 (1965) 191–250.

[21] A. Louis and E.T. Quinto, "Local Tomographic Methods in SONAR", in Surveys on Solution Methods for Inverse Problems, Ed. D. Colton, H. W. Engl, A.K. Louis, J.R. McLaughlin and W. Rundell, Springer Verlag, New York, 2000.

[22] S. Nilsson, "Application of fast backprojection techniques for some inverse problems of integral geometry", Linköping Studies in Science and Technology, Dissertation No. 499 (1997).

[23] C. J. Nolan, "Scattering near a fold caustic", in SIAM J. App. Math. Vol. 61 (2000) 659–672.

[24] C. J. Nolan and M. Cheney, "Synthetic Aperture Inversion", Inverse Problems 18 (2002) 221–236.

[25] C. J. Nolan and M. Cheney, "Synthetic Aperture inversion for non-flat topography", Proceedings, 4th European Conference on Synthetic Aperture Radar, VDE Verlag GMBH, Berlin, 2002.

[26] F. Natterer, The Mathematics of Computerized Tomography, Wiley, New York, 1986.

[27] C. J. Nolan and W. W. Symes, "Global solution of a linearized inverse problem for the acoustic wave equation", Comm. in P.D.E., Vol. 22 (1997) 919–952.

[28] A.V. Oppenheim and R.W. Shafer, Digital Signal Processing, Prentice-Hall, Englewood Cliffs, New Jersey, 1975.

[29] K.E. Oughstun and G.C. Sherman, Electromagnetic Pulse Propagation in Causal Dielectrics, Springer, New York, 1994.

[30] E.T. Quinto, "Singularities of the X-ray transform and limited data tomography in R^2 and R^3", SIAM J. Math. Anal., 24(1993), 1215-1225.

[31] T.M. Roberts and P.G. Petropoulos, "Asymptotics and energy estimates for electromagnetic pulses in dispersive media", J. Opt. Soc. Am. A 13(1996) 1204–1217.

[32] F. Treves, Basic Linear Partial Differential Equations, Academic Press, New York, 1975.

[33] F. Treves, Introduction to Pseudodifferential and Fourier Integral Operators, volumes I and II, Plenum Press, New York, 1980.

[34] L.J. Ziomek, Underwater Acoustics: A Linear Systems Theory Approach, Academic Press, Orlando, 1985.